The Influence of Unsaturated Hydrocarbon Ligands on The Stabilization of Platinum Tetramer

Mikail Aslan[1,] , Zihni Öztürk[1], Ali Sebetci

[1]*Physics Engineering Department, Gaziantep University, Gaziantep, Turkey*

Cite this article as:

Aslan, M., Öztürk, Z. & Sebetci, A. J Clust Sci (2014) 25: 1187. https://doi.org/10.1007/s10876-014-0699-z

Abstract:

In the present study, $Pt_4(CH)_n$ ($1 \leq n \leq 7$) and $Pt_4(benzene)_2$ metalorganic complexes have been investigated by performing density functional theory (DFT) within spin polarized local density approximation, generalized gradient approximation and hybrid exchange correlation functionals in terms of the geometric properties, stability and energetics, electronic properties and chemical reactivity indexes. Locally stable isomers are distinguished from transition states by vibrational frequency analysis. Our calculations indicate that $Pt_4(CH)_4$ and Pt_4benzene metal hydrocarbon complexes are the most stable structures among the studied species.

Keywords: Metal Clusters, Density Functional Theory, Stability, Energetics, Electronic Properties, hydrocarbons, unsaturated hydrocarbons, Electrophilicity, Chemical Hardness, Chemical Potential, Chemical Reactivity Indexes.

1. Introduction

Small metal nanoparticles exhibit chemical, magnetic, and optical properties that are quite different from the properties of their bulk counterparts. They are, thus, fascinating elements on the nanometer scale which are suitable to build new materials with tailored properties. In particular, metal clusters (MCs) play an important role in catalysis, medical science and nanostructured electronic devices [1-4]. Using ligands with functional groups attached to the surface metal atoms allows for the construction of functional nanoassemblies and binding the clusters to surfaces of various

substrates. Moreover, the ligand environment could significantly affect the electronic properties of the metal surfaces and the clusters themselves [5].

Colloidal MCs are cardinal for comprehension of catalytic process by formulating model catalytic systems. Using industrial catalysts supported small MCs with large variations in size and shape generally leads to face with the problems related to control the distribution of the active sites of different reaction products on the catalyst surfaces [6,7]. For this reason, in the last few decades, the study of colloidal metal particles in solution, in the nanoscale regime, with tailored properties have been carried out as the high surface volume ratio of MCs for obtaining high amounts of active sites per metal mass and most catalytic reaction changed according to the surface characteristics for given metals are important keys to take under control catalytic reaction by controlling over the nanoparticle size and shape. Thus, colloidal of metal particles of technological application due to the stabilization of metallic particles efficiently in solution have recently attracted more attention to the systems related to the synthesis of colloidal metallic particles starting from single atoms, ions, or small clusters in the model catalytic systems [8-14]. To keep the growing units from coalescence into thermodynamic equilibrium phase, the ligands could significantly affect the growing units [15-18].

Pt metal clusters are one of the ingredients of colloidal suspensions in the field of catalysis [19]. Approximately 1 nanometer sized Pt particles on chlorinated for industrial catalysts were introduced in the 1960s [20]. Lewis and co-workers contributed for the addition of Pt particles in catalytic hydrosylilation reactions [21]. After them, Colloidal metal nano particles started to use many homogenous catalytic reactions in solution, from hydrogen peroxide decomposition to cross-coupling and supported metal nanoparticles on substrate-heterogeneous catalytic reactions [22,23]. Barcaro and Fortunelli studied Pt metalorganic complexes via changing the number of metal atoms and the quantity of organic ligands. They studied small $Pt_n(ligand)_m$ (n=1 to n =3) clusters since very minute metallic clusters usually containing no more than 10 atoms, coated by solvent molecules can be produced by the metal vapor deposition technique but when producing these small metallic clusters, this technique has problem due to the low thermal stability of the solvates, which even if kept at low temperatures, decompose slowly with the formation of insoluble aggregates [24].

They tried to find possible solution for the stabilization of solvents by using ligands, which are used for inhibiting the coalescence of aggregates [14]. Mittendorfer and coworkers investigated the adsorption of the unsaturated hydrocarbons on Pt and Pd surfaces with the help of ab initio calculations [25]. Zaera and Langmuir studied species CH_3, CH_2 and CH on Pt surfaces experimentally. They showed both kinetic and spectroscopic evidence for the construction of adsorbed methyl (CH_3) and methylene (CH_2) moieties on Pt surfaces and additional kinetic data, which imply that methylidyne (CH) groups also form on the same substrate [26]. Wang and Andrews studied three Pt-C_2H_2 reaction product isomers experimentally and theoretically. They formed the vinylidene $PtCCH_2$, reacting laser-ablated Pt atoms with C_2H_2 upon co-condensation in excess argon and neon [27]. Granatier and coworkers investigated the interaction between the Pt atoms and benzene molecules using a symmetric Pt−Bz half-sandwich complex with various level of wave function theory including several functionals of the Density Functional Theory [28]. Majumdar and coworkers examined the interaction $(benzene)_n$ (n=1,2,3) with Pt and Pt_2 using a variety of the computational techniques. They found physisorbed structures and energetically lower chemisorbed species [29].

In the present study we have investigated $Pt_4(CH)_n$ ($1 \leq n \leq 7$) and $Pt_4(benzene)_2$ clusters within the framework of density functional theory (DFT). There is a number of studies available for Pt-hydrocarbon complexes, however less theoretical emphasis has been given to the platinum atoms with unsaturated hydrocarbons including equal number of hydrogen and carbon atoms. Due to the interesting catalytic properties and strong chemical structure of Pt tetrahedron, we studied Pt tetrahedron molecules with very reactive CH units to see the stability and reactivity of these structures by increasing the number of CH ligands. To understand the influence of the unsaturated hydrocarbon ligands on the stabilization of pure Pt tetramer, the geometric, energetic, electronic properties, vibrational frequency and global reactivity indexes were studied by using density functional theory within spin polarized generalized gradient approximation and hybrid exchange correlation functionals. Locally stable isomers are distinguished from transition states by vibrational frequency analysis. We present the obtained results and discuss the influence of the unsaturated hydrocarbon ligands on the stabilization of the Pt tetramer in the following sections.

2. Computational Details

NWChem 6.0 package [30] has been used to perform geometry optimizations, and to find the total energies, the vibrational frequencies, and the highest occupied and the lowest unoccupied molecular-orbital (HOMO–LUMO) gaps by DFT calculations. CRENBL [31] basis set and relativistic effective core potential (ECP) have been chosen for Pt where the outer most 18-electrons ($5s^2$ $5p^6$ $5d^9$ $6s^1$) are treated as valence to reduce the number of electrons explicitly considered in the calculations. For C and H atoms the split valence 6-31G* basis set has been employed. The reliability of the CRENBL basis set and ECP were determined by comparing atomic excitation energies with accurate all-electron calculations where maximum errors were found to be less than 0.12 eV for Pt [31]. The default convergence criteria of the code have been employed during the calculations which are $1x10^{-6}$ Hartree for energy and $5x10^{-4}$ Hartree / a_0 for energy gradient. The hybrid B3LYP [32,33] exchange-correlation functional is chosen for the transition metal cluster with hydrocarbon ligands studied in the present work. In addition, the ground state geometrical structures obtained by B3LYP hybrid functional have been re-optimized by BPW91 [34] GGA and SVWN5 [35] LDA functionals as well. The geometry optimizations without any symmetry constraints in various electronic spin multiplicities were carried out.

3. Results and Discussion

3.1 Lowest Energy Structures

The most stable structures of $Pt_4(CH)_n$ ($1 \leq n \leq 7$) hydrocarbon Pt tetramers are presented in Figure 1 and Figure 2. It can be seen in these figures that CH is adsorbed on the Pt tetramer in a molecular form with carbon instead of hydrogen bonding to platinum for each case studied in the present work. The lowest energy structure of Pt_4 is an equilateral triangular pyramid (distorted tetrahedron), which has C_{3v} point group symmetry [36]. Addition of CH ligands to the Pt tetrahedron do not change the tetrahedral configuration of the metal cluster up to the species $Pt_4(CH)_4$ for the lowest energy configurations although Pt-Pt bond distances change. For the higher sizes, tetrahedral character of the Pt tetramer is lost except the sizes n=6 and n=12. These

exceptions are reasonable since benzene is a stable molecule so that its effect on the tetrahedral character of the Pt tetramer is limited in the energetically low-lying structures. The re-examination of the most stable structures determined by using B3LYP with LDA (SVWN5) and GGA (BPW91) exchange-correlation functionals do not alter the geometric structures and bond lengths significantly.

The first CH molecule absorbed on Pt tetramer on a hollow site forming Pt_4methylidyne (see Figure 1a) is reduced the point group symmetry to C_s. Pt-Pt bond distances of the optimized structure of Pt_4methylidyne (2.63 A) slightly differ from that of pure Pt_4, which is about 2.7 A. The absorption of CH results in a small decrease of the Pt-Pt distances and therefore the three-coordinated Pt atom gets close to the plane formed by other three Pt atoms. The Pt-C bond length is 1.95 A whereas the C-H bond distance is 1.1 A. The second CH ligand prefers to be adsorbed again on another hollow site (see Figure 1b). The point group symmetry of the lowest energy structure of $Pt_4(CH)_2$ is C_{2v}. The adsorption of the second CH molecule leads to a stretch in the Pt-Pt bond lengths where the average Pt-Pt bond distance becomes 2.93 A. As a second isomer of $Pt_4(CH)_2$, Pt_4ethyne (see Figure 1c) has C_s symmetry and its energy is 0.28 eV higher than that of the structure in Figure 1b. In this structure, there are two different bond lengths between Pt and C atoms: 2.1 A and 1.9 A whereas the C-C bond distance is 1.4 A. The third isomer of $Pt_4(CH)_2$, which is the second low-lying isomer of Pt_4ethyne, is given in the Figure 1d having C_s symmetry. The binding energy of this structure is 0.44 eV higher than that of the lowest energy one. The Pt-Pt distances are 2.5 A, while Pt-C bond distance is 2 A in this structure. In summary, the chemical bond formation of two C atoms on Pt tetramer is not energetically favorable when the number of CH ligands is 2.

After the size 2, as the number of CH ligands on the Pt tetramer is increased, the new coming CH radicals prefer to form C bonds rather than to form Pt bonds only. Thus, the third CH molecule is adsorbed on a Pt-C bridge site by constructing a C-C bond of 1.42 A (see Figure 1e). Pt–Pt distances are between 2.64 A and 3.25 A in this structure. As the two Pt atoms get closer to each other the others are separated. Similarly, the forth CH goes near to the two C atoms instead of binding to the single C (see Figure 1f). This structure of $Pt_4(CH)_4$ has C_s symmetry. The average C–C bond distance is 1.43 A, which is similar to that of the previous case. There is no significant

change in the part of the structure where the single C is bonded to three Pt atoms and to the H. The average Pt-C bond distance is 2 A. After the adsorption of the fifth CH molecule, the range of the Pt-Pt distances is 2.6 A – 3.23 A, which is similar to the previous size. In the lowest energy structure of $Pt_4(CH)_5$, four C atoms and a Pt atom construct a ring. Two of the C atoms in the ring doubly bounded to each other (1.35 A). Single C-C bond distances are 1.49 A.

The lowest energy structure of $Pt_4(CH)_6$ is a Pt_4benzene (see Figure 2a) having C_s symmetry where the ring of 6 C atoms adsorbed on a triangular surface of the Pt tetramer. The Pt-C bond lengths in this structure are approximately 2.2 A. The second isomer of Pt_4benzene shown in Figure 2b has 0.06 eV higher energy than the first one. In this structure having C_{2v} symmetry, the benzene ring is adsorbed on the bridge site of Pt tetrahedron where the average Pt-Pt distance is 2.6 A. The third isomer (see Figure 2c) is in the form of $Pt_4(H)_2$benzyne whose binding energy is 0.08 eV higher relative to the lowest energy structure of Pt_4benzene. In this case, two of the six H atoms bind to Pt atoms instead of C atoms. When the seventh CH radical is added, we have a benzene ring and one CH molecule adsorbed on a hollow site in $Pt_4(CH)_7$. The average Pt-C bond distances do not change significantly. In the other lowest energy structure of $Pt_4(CH)_7$ (see Figure 2f), the benzene is isolated from Pt_4CH structure and its energy is 1.28 eV higher than the first one. When we investigate $Pt_4(benzene)_2$ structures, we identified the lowest energy structure as two benzene molecules adsorbed on different bridge sites of Pt tetramer (see Figure 3a). The average Pt-Pt bond distance in this structure is 2.57 A. The C-C (1.4 A) and Pt-C bond distances (2.2 A) are similar with those of the smaller sizes. A second isomer of $Pt_4(benzene)_2$ is given in Figure 3b which has 0.5 eV higher energy than the first isomer where one of the benzene rings is adsorbed on a bridge site while the other is adsorbed on a top side. In the third configuration (Figure 3c) we put second benzene molecule parallel to the first absorbed one and relax the structure. The second benzene remains isolated at the end of the geometry optimization, however the total binding energy of this configuration is 1.8 eV higher than the first isomer. Pt_4biphenyl is identified as a fourth isomer (Figure 3d) where an H_2 molecule separated from the rest of the structure.

3.2 Energetics and Stability

In order to predict the relative stabilities of the $Pt_4(CH)_n$ ($1 \leq n \leq 7$ and $n = 12$) structures, the binding energy per atom and the second finite difference in energies are calculated and plotted in Figure 4 and Figure 5 respectively. The binding energy per atom (*BE/n*) has been obtained in the following way:

$$BE/n = \frac{nE[C] + nE[H] + 4E[Pt] - E[Pt_4(CH)_n]}{n} \quad \text{from n = 1 to n = 11} \qquad (1)$$

where *E*[*] is the total energy of the neutral Carbon, Hydrogen, Platinum atoms and the cluster, respectively. It is clear that the binding energies per atom of the species continuously increase with the increase of the number of CH molecules (see Figure 4), which indicates that the species can constantly gain energy during the growth process as the gained energy rate slows down. The binding energy per atom of the pure platinum tetramer is 2.4 eV/atom. After the absorption of the first CH molecule, the binding energy increased rapidly to 3.7 eV/atom.

To further illustrate the stability of the species and their size dependent behaviors, we have considered the second finite difference in energies that is a sensitive quantity frequently used as a measure of the relative stability of the complexes and is often compared directly with the relative abundances determined in mass spectroscopy experiments. Moreover, clusters are especially abundant magic number sizes in mass spectra as they are most stable ones. The second finite different energies (D_n) can be calculated as

$$D_n = E_{n+1} + E_{n-1} - 2E_n \qquad (2)$$

where E_n is the total energy of the cluster $Pt_4(CH)_n$. The second finite difference (D) in energies versus cluster size plot is given in Figure 5. Due to the definition of the second finite difference in energies, we examined these energies for $Pt_4(CH)_n$ clusters from n = 2 to n = 6. The peak at the size of Pt_4benzene indicates that this species is the most stable one in the present study. $Pt_4(CH)_5$ can be considered as the least stable structure as it corresponds to a dip in the plot. Commonly, the more stable the species,

the lower reactivity of the species to absorb CH. Thus, Pt_4benzene is expected to be more abundant in mass spectra when compared to the other sizes.

$$Pt_4(CH)_n + CH \rightarrow Pt_4(CH)_{n+1}$$

reaction energies calculated by B3LYP xc-functional are given in Table I. For each n, the reaction is exothermic. The most favorable reactions are

$$Pt_4 + CH \rightarrow Pt_4CH \quad \text{and} \quad Pt_4(CH)_5 + CH \rightarrow Pt_4\text{benzene}$$

since the reaction energy for them are the least values in the Table I. On the other hand the least favorable reactions are

$$Pt_4(CH)_3 + CH \rightarrow Pt_4(CH)_4 \quad \text{and} \quad Pt_4(CH)_4 + CH \rightarrow Pt_4(CH)_5$$

since they both, see Table I, have the highest reaction energies. These results are in consistent with second finite difference in total energies as they also indicate that Pt_4benzene is favorable but $Pt_4(CH)_5$ is not.

The reaction energies calculated by employing BPW91 xc-functional is slightly different from those of B3LYP. For instance, the reaction energy of

$$Pt_4CH + CH \rightarrow Pt_4(CH)_2$$

is -6.5 eV and -6.1 eV by BPW91 and B3LYP, respectively. However, it is obtained that the choice of the xc-functional does not affect the trend for the favorable reactions.

3.3 Electronic Properties

Vertical ionization potentials (IP) and electron affinities (EA) are calculated as the total energy difference of neutral, anionic and cationic species in the following way:

$$IP[Pt_4(CH)_n] = E[Pt_4(CH)_n^+] - E[Pt_4(CH)_n] \qquad (5)$$

$$EA[Pt_4(CH)_n] = E[Pt_4(CH)_n] - E[Pt_4(CH)_n^-] \quad (6)$$

Here, $E[Pt_4(CH)_n]$, $E[Pt_4(CH)_n^-]$ and $E[Pt_4(CH)_n^+]$ refer to total energy of the neutral, anionic and cationic clusters respectively. The energy of the highest occupied molecular orbital (HOMO) can be considered as a measure of the tendency of the structure to give an electron, whereas the energy of the lowest unoccupied molecular orbital (LUMO) as a measure of the tendency of the structure to accept an electron. The higher the HOMO energy, the higher is the tendency to give an electron, and the lower the LUMO energy, the higher is the tendency to accept an electron. A large HOMO-LUMO gap has been considered as significant requirement for chemical stability [37]. Calculated ionization potentials (IP), electron affinities (EA), HOMO-LUMO gaps and lowest and highest vibrational frequencies are given in the Table 2. We have also given the 3D plots of the frontier orbitals, HOMO and LUMO for $Pt_4(CH)_4$ and Pt_4benzene in Figure 6.

The Pure Pt tetramer has 1 eV HOMO-LUMO gap energy. The adsorption of CH units on Pt atoms leads to change the gap energy between 0,4 and 1.4 eV. The Pt_4methylidyne has the lowest HOMO-LUMO gap with the value of 1.4 eV in our study whereas the highest gap (2.4 eV) belongs to $Pt_4(CH)_4$. Pt_4benzene possesses a large HOMO-LUMO gap (2.3 eV) as well, which is consistent with its high stability. $Pt_4(benzene)_2$ is one of those having small HOMO-LUMO gap within the studied structures, which indicates high chemical activity similar to Pt_4CH. The lowest EA is obtained for $Pt_4(CH)_3$ cluster, while the highest EA in the present study is obtained for Pt_4benzene and $Pt_4(CH)_7$ (2.1 eV). The $Pt_4(CH)_4$ cluster has the highest IP with the value of 9.4 eV. The lowest and the highest vibrational frequencies for all of the clusters change between 15 to 3213 cm^{-1}.

3.4 DFT Chemical Reactivity Descriptors

In this section, we center our attention on the characterization of the species we have studied in terms of reactivity descriptors such as chemical potential (μ), chemical hardness (η) and electrophilicity index (w). Those quantities are displayed in Table 3. We calculated electronic chemical potential and chemical hardness according to the finite difference approximation [38]:

$$\mu = -(1/2)(IP+EA) \quad (7)$$

$$\eta = -(1/2)(IP-EA) \quad (8)$$

μ determines the escaping tendency of electrons from an equilibrium system and η can be defined as a resistance to the charge transfer [39]. The global electrophilicity index is derived from the chemical potential and hardness as the following [38]:

$$w = \mu^2/2\eta \quad (9)$$

w measures the stabilization in energy as the environment gives systems extra electronic charges.

Global indicators constitute good indexes to describe the reactivity and the intrinsic electronic properties of the system, and show the feasibility of the chemical change. It is harder to lose an electron but easier to take another one when μ becomes more negative [39]. It is observed in Table 3 that $Pt_4(CH)_4$ has the lowest chemical potential of -5.1 eV. η generally shows parallel tendency with chemical potential descriptors. Accordingly, $Pt_4(CH)_4$ is the hardest (4.3 eV) one in our calculations. The smallest chemical hardness belongs to Pt_4benzene with the value of 1.95 eV. According to the ω values given in Table 3, the $Pt_4(CH)_7$ is the most susceptible from the external environment. The electrophilicity index, which can be one of the essential parameter for the selection of a catalyzer, shows oscillating behavior in Table 3.

4. Conclusion

In the present study, we have performed spin-polarized density functional theory calculations to study the interaction of the $Pt_4(CH)_n$ (n = 1 to 7 and n =12) metalorganic complexes by varying the number of CH ligands. The geometric properties, energetics and stability, electronic properties and chemical reactivity indexes have been discussed. From the analyses of the results, the following conclusions can be drawn: First of all, during the growth process with CH on Pt tetramer, atop site adsorption of CH to the species is not energetically favorable. CH

is adsorbed on the tetramer in the molecular form with carbon instead of hydrogen bonding to platinum. The first and second adsorptions of CH ligands occur on the hollow sides of the Pt tetramer. After the size 2, as the number of CH ligands on the Pt tetramer is increased, CH radicals start to form C bonds. This trend continues up to the size 6. The lowest energy configuration of $Pt_4(CH)_6$ becomes a Pt_4benzene where the ring of 6 C atoms adsorbed on a triangular surface of the Pt tetramer. For $Pt_4(benzene)_2$ structures, the lowest energy structure is obtained as two benzene molecules adsorbed on different bridge sites of the Pt tetramer. Finally, regarding the relative stability criteria, reaction energies, chemical reactivity descriptor indexes and electronic properties of the studied clusters, $Pt_4(CH)_4$ and Pt_4benzene metal unsaturated hydrocarbon complexes are found to be the most stable species among the studied sizes.

Referrences

[1] F. Baletto, R. Ferrando (2005). Rev. Mod. Phys, **77**, 371.

[2] Kuppusamy and Murugan C. Kuppusamy, K. Murugan (2009). Int. J. Integr. Biol., **5** (2), 75–81.

[3] I. Robinson, S. Zacchini, L.D. Tung, S. Maenosono, N.T.K. Thanh (2009). Chemistry of Materials **21**, 3021.

[4] S. Shylesh, V. Schuneman, W.R. Thiel, Angew (2010). Chem. Int. Ed. **49**, 3428.

[5] Satyender Goel, Kirill A. Velizhanin , Andrei Piryatinski , Sergei Tretiak and Sergei A. Ivanov (2010). J. Phys. Chem. Lett. **1** (6), 927–931.

[6] G. Ertl, D. Prigge, R. Schloegl and M. Weiss, J. Catal (1983). **79**, 359–377.

[7] J. Yang, V. Tschamber, D. Habermacher, F. Garin and P. Gilot (2008). Appl. Catal., B, **83**, 229-239.

[8] Schmid G. (1996). Applied homogeneous catalysis with organometallic compounds, vol **2**, Wiley, Wienheim, 636–644.

[9] Bonnemann H, Brijoux W (1996). Advanced catalysts and nanostructured materials, chap 7. Academic Press, San Diego, 165–196.

[10] Herrmann WA, Cornils B (1996) Applied homogeneous catalysis with organometallic compounds, vol 2. Wiley, Wienheim, 1171–1172.

[11] Gotz M, Wendt H (1998). Electrochim Acta **43**, 3637.

[12] Schmidt TJ, Noeske M, Gasteiger HA, Behm RJ, Britz P, Brijoux W, Bonnemann H (1997). Langmuir **13**, 2591.

[13] Schmidt TJ, Noeske M, Gasteiger HA, Behm RJ, Britz P, Bonnemann H (1998). J Electrochem Soc **145**, 925.

[14] Giovanni Barcaro, Alessandro Fortunelli (2009). Theor Chem Acc **123**, 317-325.

[15] Toshima N, Yonezawa T (1998). New J Chem **22**, 1179.

[16] Aiken III JD, Finke RG (1999). J Mol Catal A **145**, 1.

[17] Leisner T, Rosche C, Wolf S, Granzer F, Woste L (1996). Surf Rev Lett **3**,1105.

[18] Faraday M (1857). Philos Trans R Soc Lond **147**,145.

[19] Chun-Jiang Jia and Ferdi Schüth (2011). Phys. Chem. Chem. Phys **13**, 2457-2487.

[20] V. Haensel and H. S. Bloch (1964). Platinum Met. Rev **8**, 2–8.

[21] L. N. Lewis and N. Lewis (1986). J. Am. Chem. Soc. **108**, 7228–7231.

[22] J. S. Bradley (1994). Clusters and colloids, ed. G. Schmid, VCH, Weinheim, 459.

[23] M. T. Reetz and W. Helbig (1994). J. Am. Chem. Soc. **116**, 7401–7402.

[24] Blackborrow JR, Young D (1979). Metal vapor synthesis. Springer, NewYork

[25] F. Mittendorfer, C. Thomazeau, P. Raybaud, and H. Toulhoa (2003). J. Phys. Chem. B **107** (44), 12287-12295.

[26] Zaera, F. Langmuir (1991), Reversibility of C1 Hydrogenation-Dehydrogenation Reactions on Platinum Surfaces under Vacuum, 7, 1998.

[27] X. Wang and and L. Andrews (2004). J. Phys. Chem. A **108** (22), 4838-4845

[28] J. Granatier, M. Dubecký, P. Lazar, M. Otyepka, and P.Hobza (2013). J. Chem. Theory Comput. **9** (3), 1461-1468

[29] D. Majumdar, S. Roszak and K Balasubramanian, (2001). J. Chem. Phys. **114**, 10300-10310.

[30] E.J. Bylaska, W.A. de Jong, K. Kowalski, T.P. Straatsma, M. Valiev, D. Wang, E. Apra, T.L. Windus, S. Hirata, et al.(2006), NWChem, A Computational Chemistry Package for Parallel Computers, Version 5.0, Pacific Northwest National Laboratory, Richland, Washington 99352-0999, USA.

[31] M.M. Hurley, L.F. Pacios, P.A. Christiansen, R.B. Ross, W.C. Ermler (1986), Journal of Chemical Physics 84 6840.

[32] A.D. Becke (1988), Physical Review A 38 3098;
A.D. Becke (1993), Journal of Chemical Physics 98 5648.

[33] C. Lee, W. Yang, R.G. Parr (1988), Physical Review B 37 785.

[34] J.P. Perdew, K. Burke, M. Ernzerhof (1996), Physical Review Letters 77 3865.

[35] S.J. Vosko, L. Wilk, M. Nusair (1980), Canadian Journal of Physics 58 1200

[36] Sebetci A, (2006), Chem. Phys. **331**, 9; (2009), Phys. Chem. Chem. Phys. **11**, 921.

[37] Jun Li, Xi Li, Hua-Jin Zhai, and Lai-Sheng Wang (2003). Science **299** (5608), 864-867.

[38] R. Rarr, R.G. Pearson (1983), J. Am. Chem. Soc. **105**, 7512-7516.

[39] C.L. Heredia, V. Ferraresi-Curotto, M.B. López (2012). Comp. Mater. Sci. **53**, 18-24.

Figure Captions

Figure 1 The lowest energy structures and some isomers of $Pt_4(CH)_n$ (n = 1 to 5) clusters

Figure 2 The lowest energy structures and some isomers of $Pt_4(CH)_6$ and $Pt_4(CH)_7$ clusters

Figure 3 The low lying isomers of $Pt_4(benzene)_2$ clusters

Figure 4 The binding energies per atom for $Pt_4(CH)_n$ (n = 1 to 7 and n=12) clusters

Figure 5 The second finite difference in energies for $Pt_4(CH)_n$ (n =2 to 6) clusters

Figure 6 HOMO and LUMO of $Pt_4(CH)_4$ and Pt_4benzene clusters

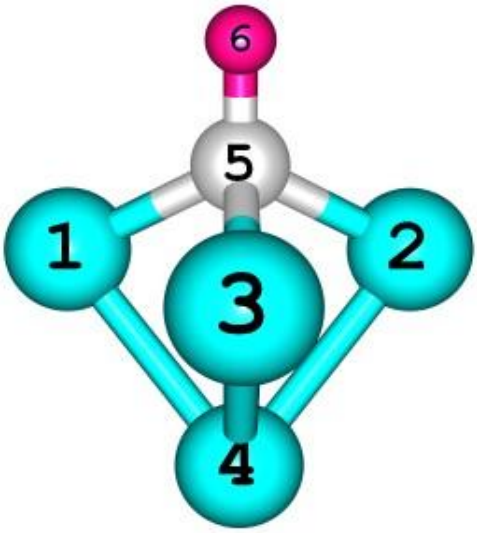

(a) Pt_4methylidyne

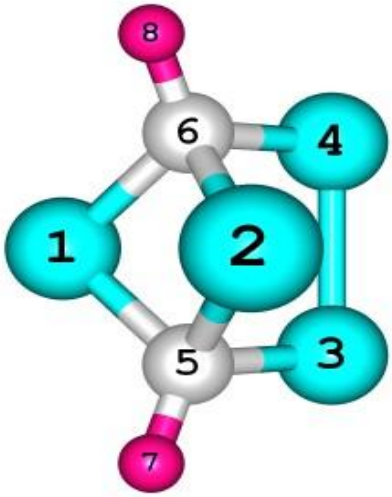

(b) $Pt_4(CH)_2$ 0 eV

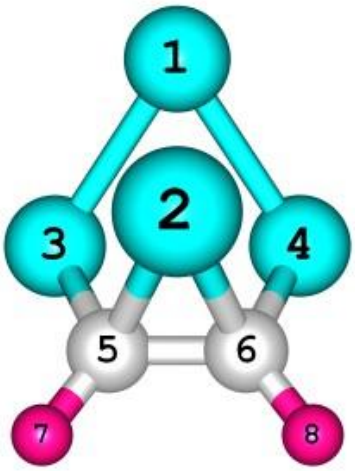

(c) Pt_4ethyne-1 0.28 eV

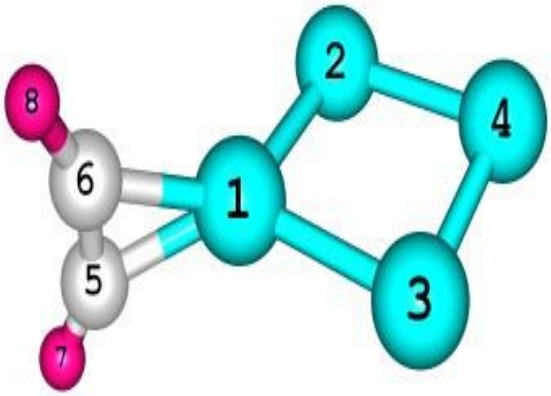

(d) Pt_4ethyne-2 0.44 eV

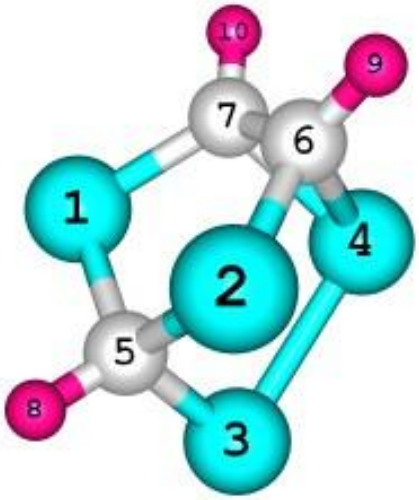

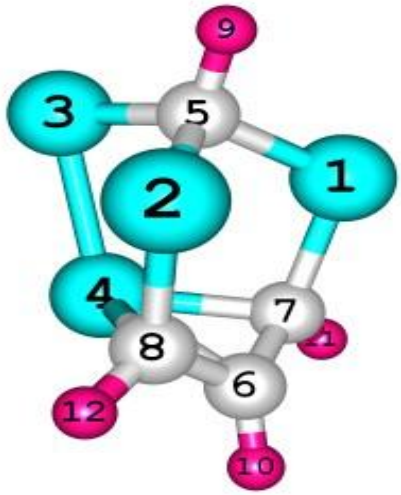

(e) $Pt_4(CH)_3$	(f) $Pt_4(CH)_4$
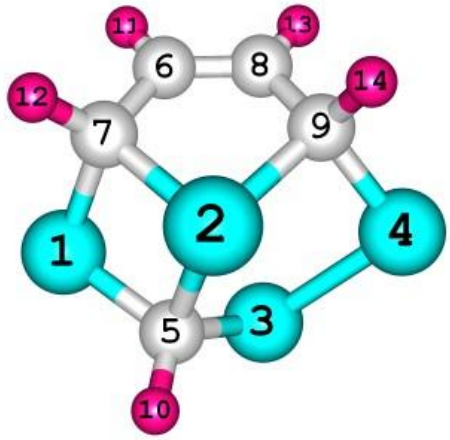	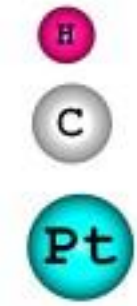
(g) $Pt_4(CH)_5$	

Figure 1 The lowest energy structures and some isomers of $Pt_4(CH)_n$ (n = 1 to 5) clusters

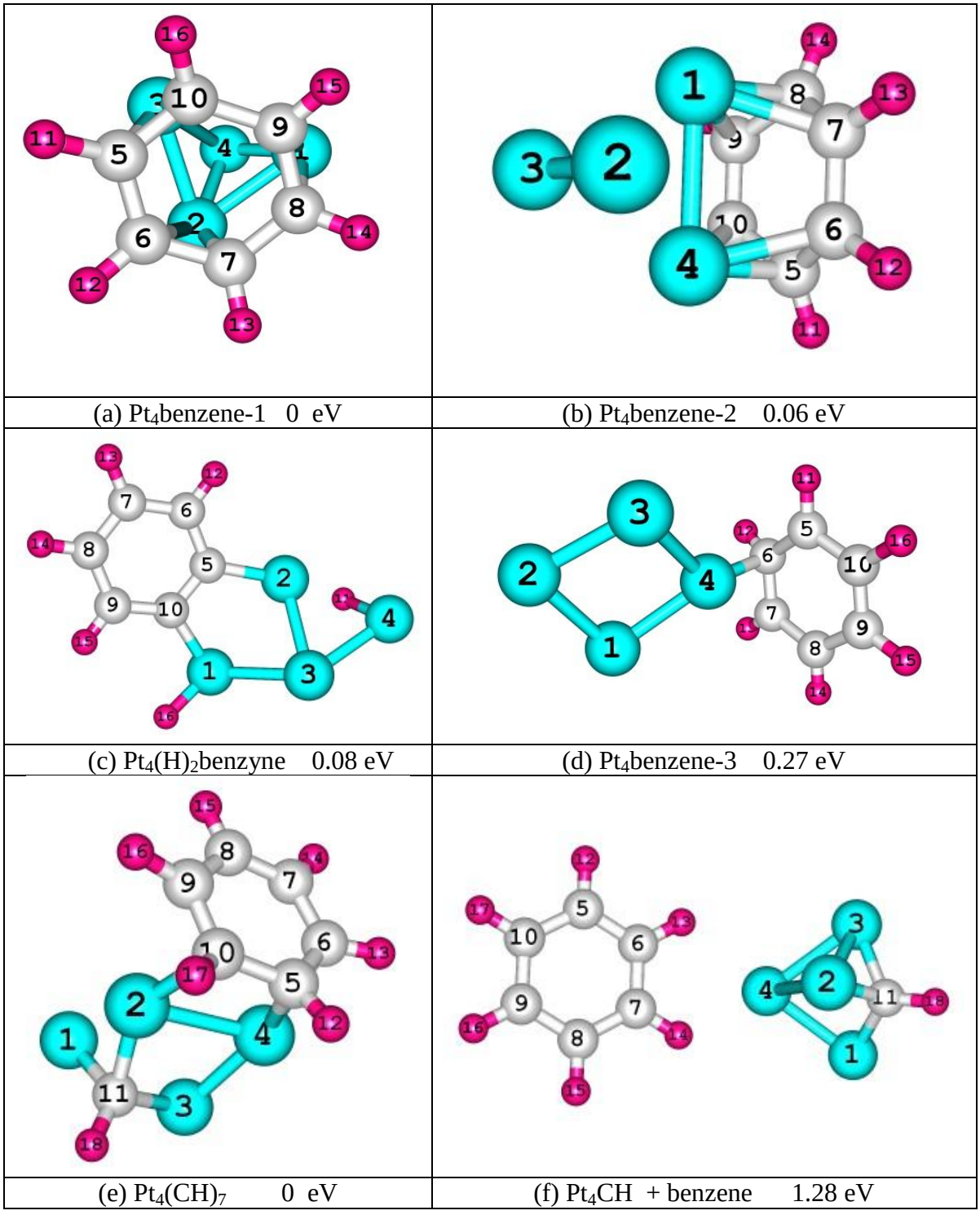

(a) Pt_4benzene-1 0 eV | (b) Pt_4benzene-2 0.06 eV

(c) $Pt_4(H)_2$benzyne 0.08 eV | (d) Pt_4benzene-3 0.27 eV

(e) $Pt_4(CH)_7$ 0 eV | (f) Pt_4CH + benzene 1.28 eV

Figure 2 The lowest energy structures and some isomers of $Pt_4(CH)_6$ and $Pt_4(CH)_7$ clusters

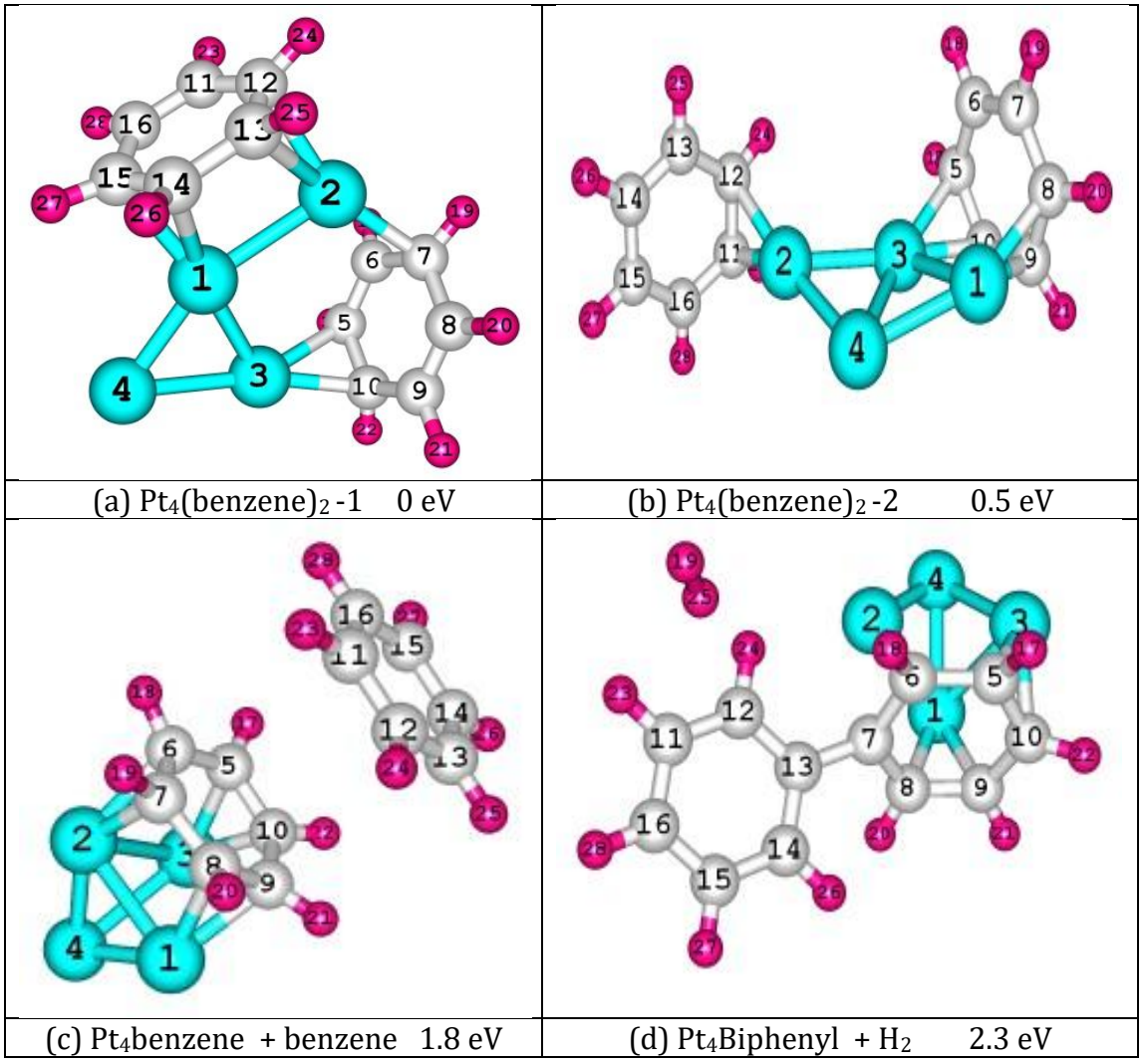

(a) $Pt_4(benzene)_2$ -1 0 eV

(b) $Pt_4(benzene)_2$ -2 0.5 eV

(c) Pt_4benzene + benzene 1.8 eV

(d) Pt_4Biphenyl + H_2 2.3 eV

Figure 3 The low lying isomers of $Pt_4(benzene)_2$ clusters

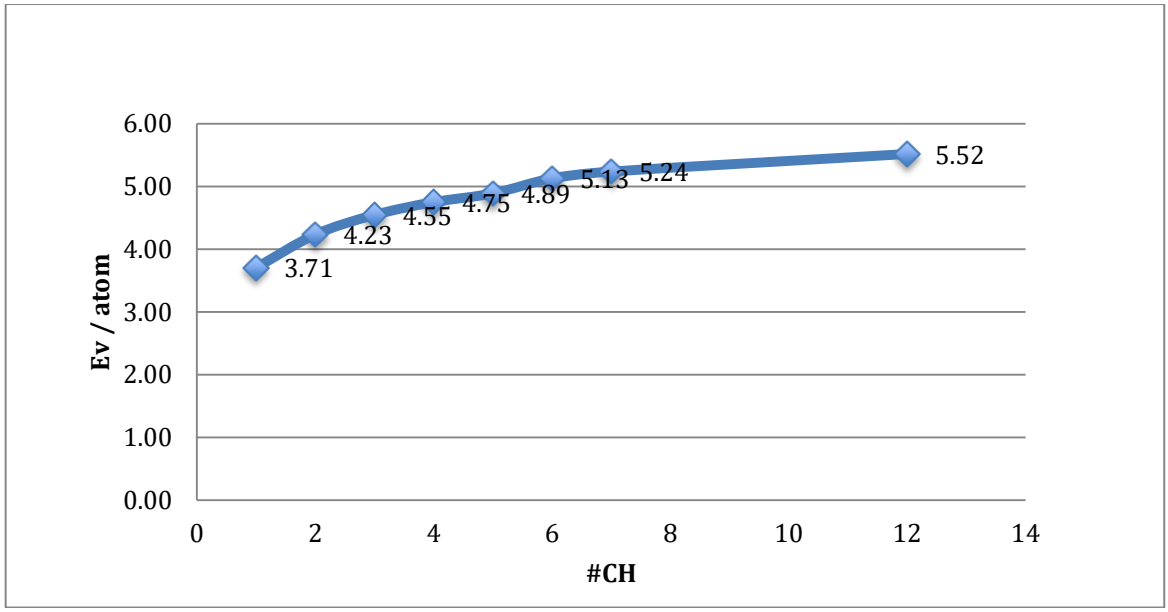

Figure 4 The binding energies per atom for $Pt_4(CH)_n$ (n = 1 to 7 and n=12) clusters

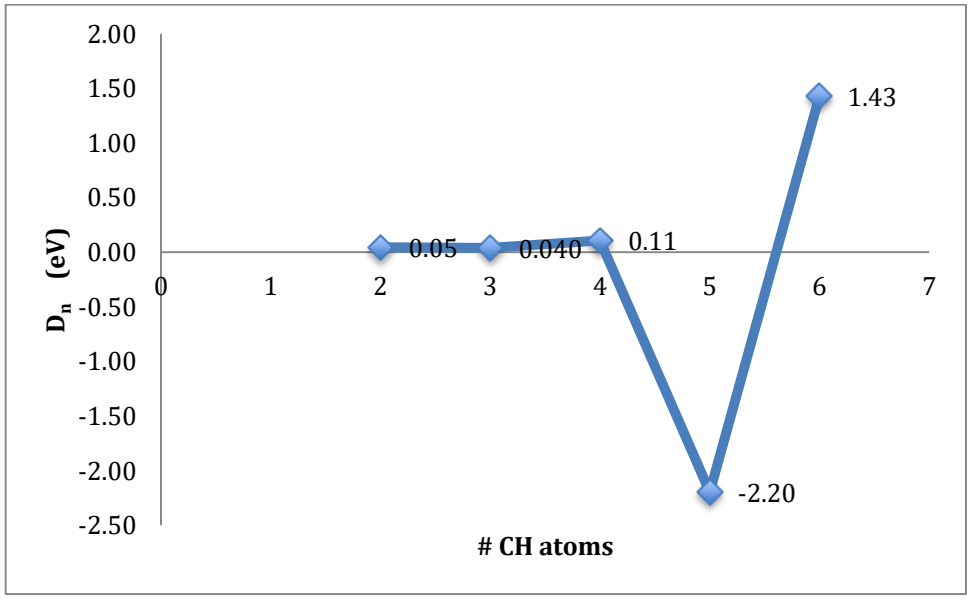

Figure 5 The second finite difference in energies for $Pt_4(CH)_n$ (n =2 to 6) clusters

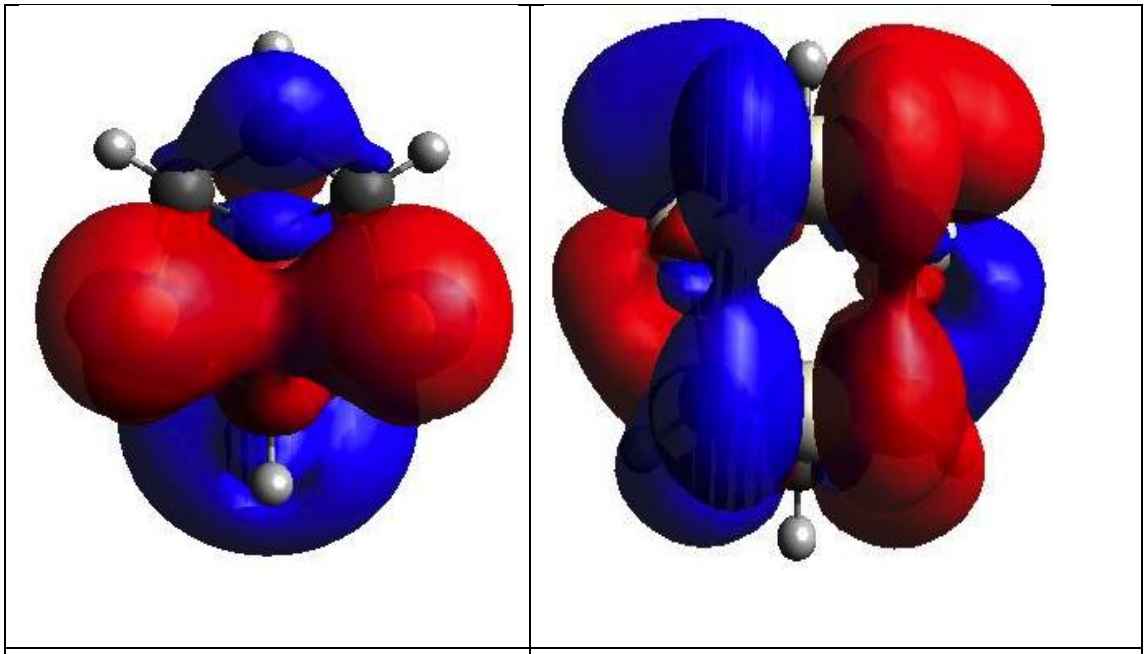

(a) HOMO of $Pt_4(CH)_4$ | (b) LUMO of $Pt_4(CH)_4$

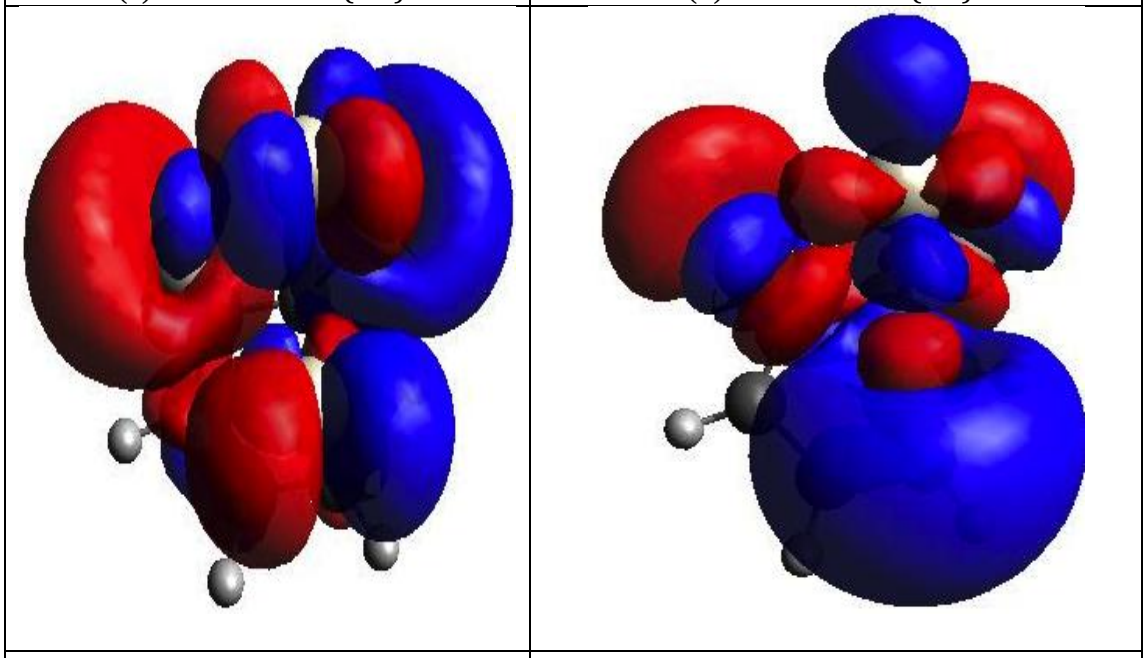

(c) HOMO of Pt_4benzene | (d) LUMO of Pt_4benzene

Figure 6 HOMO and LUMO of $Pt_4(CH)_4$ and Pt_4benzene clusters.

Table 1 Reaction Energies with Two XC functionals B3LYP and BW91 respectively

Reaction	ΔE_1 (eV)	ΔE_2 (eV)
Pt_4 + CH $\rightarrow$ Pt_4 methylidyne	-7.12	-7.51
Pt_4CH + CH $\rightarrow$ $Pt_4(CH)_2$	-6.11	-6.54
$Pt_4(CH)_2$ + CH $\rightarrow$ $Pt_4(CH)_3$	-6.06	-6.30
$Pt_4(CH)_3$ + CH $\rightarrow$ $Pt_4(CH)_4$	-6.02	-6.36
$Pt_4(CH)_4$ + CH $\rightarrow$ $Pt_{4(}CH)_5$	-5.92	-6.78
$Pt_{4(}CH)_5$ + CH $\rightarrow$ Pt_4benzene	-8.11	-7.71
Pt_4benzene + CH $\rightarrow$ $Pt_4(CH)_7$	-6.68	-6.76

Table 2 The Electronic Properties of $Pt_4(CH)_n$ (n=1 to 7 and n = 12) Clusters

Cluster	EA (eV)		IP (eV)		BE per atom (eV/atom)		HOMO-LUMO gap (eV)		Lowest and highest vibrational frequencies (cm^{-1})	
	B3LYP	**BPW91**	**B3LYP**	**BPW91**	**B3LYP**	**BPW91**	**B3LYP**	**BPW91**	**B3LYP**	**BPW91**
Pt_4methylidyne	1.52	1.59	6.72	6.77	3.71	6.21	1.43	0.58	60-2208	46-2943
$Pt_4(CH)_2$	1.82	1.86	7.01	6.90	4.23	5.92	2.01	0.75	45-3017	43-2950
Pt_4ethyne	2.10	2.00	6.26	6.43	4.20	5.86	1.46	0.48	15-3100	57-3051
$Pt_4(CH)_3$	0.00	1.69	6.41	6.38	4.55	5.72	2.34	1.19	57-3098	50-3026
$Pt_4(CH)_4$	0.78	0.90	9.38	6.83	4.75	5.59	2.41	1.14	59-3174	29-3121
$Pt_4(CH)_5$	1.82	1.82	6.14	6.87	4.89	5.53	2.20	1.47	37-3185	63-3069
Pt_4benzene	2.09	2.02	5.99	6.10	5.13	5.55	2.28	0.05	66-3213	72-3137
$Pt_4(CH)_7$	2.14	2.12	6.40	6.38	5.24	5.50	1.96	0.83	32-3087	29-3149
$Pt_4(benzene)_2$	1.50	1.53	6.06	6.07	5.52	5.37	1.93	0.43		

Table 3 The Chemical Reactivity Descriptors Indexes of $Pt_4(CH)_n$ (n=1 to 7 and n= 12) Clusters in eV

Clusters	Chemical Potential (μ)		Chemical Hardness (□)		Electrophilicity Index (w)	
	B3LYP	BPW91	B3LYP	BPW91	B3LYP	BPW91
Pt_4methylidyne	-4.12	-4.18	2.60	2.59	3.27	3.37
$Pt_4(CH)_2$	-4.42	-4.38	2.60	2.52	3.75	3.80
Pt_4ethyne	-4.18	-4.22	2.08	2.22	4.21	4.01
$Pt_4(CH)_3$	-3.21	-4.03	3.21	2.35	1.60	3.46
$Pt_4(CH)_4$	-5.08	-3.86	4.30	2.96	3.00	2.52
$Pt_4(CH)_5$	-3.98	-4.34	2.16	2.52	3.66	3.74
Pt_4benzene	-4.04	-4.06	1.95	2.04	4.19	4.03
$Pt_4(CH)_7$	-4.27	-4.25	2.13	2.13	4.29	4.24
$Pt_4(benzene)_2$	-3.78	-3.80	2.28	2.27	3.14	3.18